Energy-Efficient Channel-Dependent Cooperative Relaying for the Multiuser SC-FDMA Uplink

Jiayi Zhang, *Student Member, IEEE*, Lie-Liang Yang, *Senior Member, IEEE*, and Lajos Hanzo, *Fellow, IEEE*

***Abstract*—In this paper, we exploit the benefits of combining the diversity gains that arise from cooperation, multiple propagation paths, and opportunistic relaying (OR) of multiple users. Our goal is to improve the energy efficiency of the amplify-and-forward (AF) single-relay-assisted single-carrier frequency-division multiple-access (SC-FDMA) uplink, where the single relay considered may support a single user or may be shared by multiple users who communicate over dispersive channels subject to large-scale fading. Based on the proposed amalgam of single-tap frequency-domain equalization (FDE) and a diversity-combining-aided receiver that relies on the minimum mean-square error (MMSE) criterion, three different relay selection schemes designed for either single-user or multiuser relaying scenarios are investigated, when combined with source/relay power sharing, which employ imperfect power control. Our results demonstrate that, at a bit error ratio (BER) of 10^{-4}, the proposed receiver can save 2 dB power by achieving a higher cooperative diversity gain than the conventional receiver. Moreover, a beneficial energy efficiency improvement may be achieved when the cooperative regime operates at $E_b/N_0 < 0$. Most importantly, when the shadowing variance is increased from 4 dB to 8 dB, the energy consumption gain gleaned from our multiuser and multiaccess relay selection schemes may increase to $4 \sim 9$, compared with the direct transmission in the absence of shadowing at $E_b/N_0 = -10$ dB.**

***Index Terms*—Cooperative communications, diversity combining, energy efficiency, frequency-domain equalization (FDE), opportunistic relaying (OR), power allocation, relay selection, single-carrier frequency-division multiple-access (SC-FDMA).**

I. Introduction

COOPERATIVE communication [1] systems have attracted the attention of both academia and industry in recent years, because they can achieve a diversity gain in *large-scale fading* environments by sharing the resources of the cooperating user terminals. This case allows us to jointly exploit the benefits of both *time* and *frequency diversity* to mitigate the deleterious effects of wireless propagation and/or to increase the attainable system throughput and *energy efficiency* [2]–[5]. Recently, the family of *cooperative-diversity*-oriented *multiple-access* (MA) and distributed *multiple-input–multiple-output* (MIMO)-aided multiplexing techniques has been invoked to design the *uplink* of advanced cooperative cellular networks [6]–[8]. Furthermore, the cooperative concepts have been extended to broadband systems by designing techniques for mitigating the effects of *frequency-selective fading* with the aid of *multicarrier* (MC) techniques associated with appropriate *source/relay power sharing* [9], [10].

From a *multiuser* (MU) network point of view, the cooperative link sharing from the *source mobile terminals* (MTs) to the *base station* (BS) can be determined by choosing the single or multiple *relays* [11] from a cluster of idle MTs. In general, the *random relay selection* (RRS) philosophy allows the BS to randomly appoint a relay without any channel knowledge, but in this case, simultaneous gains from relaying path and selection diversity are limited. By contrast, the so-called *distance-dependent relay selection* (DD-RS) [8] policy is based on the distance from the relay to the source MT or BS; hence, *relay candidates* (RCs) that benefit from a high path gain may experience deep shadowing and fast fading. However, the *channel-dependent relay selection* (CD-RS) regime benefits from a certain *degree of freedom* in terms of selecting the cooperating MT by monitoring the instantaneous channel conditions in a distributed scenario, including the associated path-loss, shadowing, and *multipath fading* effects. Therefore, it is also known as *opportunistic relaying* (OR) [12], which can exploit the selection diversity, which we refer to as *MU diversity*, that arises from appropriate relay selection [13]–[16].

The *single-carrier frequency-division multiple-access* (SC-FDMA) technique [17] was adopted for the uplink of the *Third-Generation Partnership Project* (3GPP) *Long-Term Evolution* (LTE) standard [18]. In recent years, Falconer *et al.* [19], [20] have investigated the SC modulation with *linear* and nonlinear *frequency-domain equalization* (FDE) [21] techniques for broadband receiver solutions. Furthermore, the principle of SC-FDMA and its *discrete Fourier transform* (DFT) spread *orthogonal frequency-division multiplexing* (OFDM) [22] transmitter structures using either interleaved or localized subband mapping schemes were studied in [23] and [24]. SC-FDMA was shown to avoid the *multiuser interference* (MUI) imposed by the *cooperative sources* and *relays* upon the uplink receiver of the BS while maintaining a low *peak-to-average power ratio* (PAPR). The *amplify-and-forward* (AF) *single-relay*-assisted SC-FDMA uplink scheme was proposed in [25] for both *single dedicated relaying* (SDR), with each dedicated relay aiding a single user, and *single shared relaying* (SSR), with a single

Manuscript received April 12, 2010; revised July 24, 2010, October 18, 2010, and December 20, 2010; accepted December 29, 2010. Date of publication January 10, 2011; date of current version March 21, 2011. The work reported in this paper has formed part of the Core 5 Research Programme of the Virtual Centre of Excellence (VCE) in Mobile and Personal Communications, Mobile VCE, www.mobilevce.com, whose funding support, including that of EPSRC, is gratefully acknowledged. Fully detailed technical reports on this research are available to Industrial Members of Mobile VCE. This work was presented in part at the 2010 IEEE Spring Vehicular Technology Conference, May 16–19, 2010, Taipei, Taiwan. The review of this paper was coordinated by Dr. D. W Matolak.

The authors are with the School of Electronics and Computer Science, University of Southampton, SO17 1BJ Southampton, U.K. (e-mail: jz07r@ecs.soton.ac.uk; lly@ecs.soton.ac.uk; lh@ecs.soton.ac.uk).

Color versions of one or more of the figures in this paper are available online at http://ieeexplore.ieee.org.

Digital Object Identifier 10.1109/TVT.2011.2104985

0018-9545/$26.00 © 2011 IEEE

shared relay aiding all the active users. The AF relay estimates the received power of each subband and equalizes the power differences of the subbands, which corresponds to *subband-based equalization*. By inheriting the features of the SC-FDMA system that invokes a DFT-spread (S)-OFDM-style transmitter, this relaying scheme carries out the so-called *subband remapping* [25] at the relay to remove the effects of both noise and interference inflicted by other relays without changing the frequency band of the signals transmitted from the source MT. One OFDM scheme that relies on time-division-multiplexing-based cooperative relaying and uses *minimum mean-square error* (MMSE)-assisted *frequency-domain equalizers* (FDEs) was proposed in [26]. However, in [25] and [26], MMSE-FDE was independently operated in the context of the *direct* and *relaying branches*, which were then combined with the aid of a *time-domain* (TD) *equal-gain combiner* (EGC) [27]. In [28]–[32], linear and adaptive FDEs that rely on *diversity-combining* schemes were invoked for multiple-antenna-aided SC- or OFDM-based block transmissions. Furthermore, in [33]–[35], the receive diversity-combining techniques that were designed for SC-FDMA and rely on cooperative relays were considered by stipulating the idealized simplifying assumption that the relays perfectly demodulate/detect the source signals before forwarding them.

- Although the authors of the aforementioned articles proposed various FDEs amalgamated with diversity-combining schemes designed for MIMOs, for OFDM, or for relaying systems, due to the potentially nonwhite noise contribution of AF cooperative relaying, the equivalent noise encountered at the BS is also nonwhite. Furthermore, we typically encounter a different noise power at each cooperative branch; hence, the conventional *maximum ratio combiner* (MRC) [27] becomes suboptimal, unless *noise whitening* is adopted. To the best of our knowledge, no article investigated the joint design of the linear single-tap FDE amalgamated with the diversity combiner of the direct and relayed link using noise whitening for the AF-relaying-assisted SC-FDMA uplink.
- Because finite-delay *power control* schemes that use a discrete stepsize cannot perfectly perform in realistic wireless uplink transmissions, the source/relay power sharing employed imposes a time-varying level of *power control error* (PCE) [36]. In [6], [9], [10], and [13], various relay selection and source/relay power allocation schemes were proposed and studied, but no such schemes were designed for the cooperative SC-FDMA uplink under imperfect power control, with the goal of improving energy efficiency.
- The authors of [37]–[39] studied various relay selection schemes designed for OFDM and CDMA systems subjected to both path-loss and multipath fading. However, cooperative relaying allows the collaborating mobiles to avoid the typical diversity gain erosion imposed by shadowing effects as a benefit of their geographically separated locations. Hence, we embarked on investigating the relay-selection-induced benefits of our system in the presence of shadow fading, whose impact on the energy efficiency of cooperative SC-FDMA systems has not been documented in the open literature.

In this paper, we propose and investigate an energy-efficient opportunistic cooperative relaying scheme designed for SC-FDMA arrangements. The joint frequency-domain equalization and combining (JFDEC)-aided receiver is designed to detect the cooperative SC-FDMA uplink signals. In this paper, both single-user relay selection (SU-RS) and multiuser relay selection (MU-RS), as well as multiple-access relay selection (MA-RS), are considered in diverse opportunistic cooperative relaying scenarios. By contrast, in [40], only the SU-RS and MU-RS schemes based on the JFDEC receiver were studied in the context of the SDR topology.

- Furthermore, in contrast to the open literature, our focus is mainly on the analysis of the energy efficiency of the cooperative SC-FDMA system, where energy efficiency is quantified in terms of the energy consumption ratio (ECR) and energy consumption gain (ECG), as defined in [41].
- The MMSE-criterion-aided JFDEC scheme considered in [40] is further detailed, which amalgamates the design of the linear single-tap FDE and the diversity combiner of the direct and relayed link with noise whitening applied at the BS.
- Furthermore, we investigate the MA-RS scheme created by generalizing the SU-RS and MU-RS philosophies developed from the context of the SDR-to-SSR topologies, where the relative merits of the SU-RS, MU-RS, and MA-RS schemes are discussed in light of their complexity, and the effects of *imperfect power control*[1] are also quantified.
- In addition, we demonstrate that, upon encountering a realistic propagation *path-loss* and *shadowing*, significant *relaying* and *selective diversity gains* are attainable through the proposed *optimal power allocation (OPA)*[2]-aided SU-RS, MU-RS, and MA-RS schemes, which allows us to reduce the required *signal-to-interference-plus-noise ratio* (SINR) for improving the performance of ECG. Finally, the practicability and feasibility of various power-sharing schemes are discussed in terms of their computational complexity.

This paper is organized as follows. In Section II, the system model of the cooperative SC-FDMA uplink is presented. In Sections III and IV, we outline the improved signal detection and investigate the relay selection schemes, respectively. The attainable performance of our proposed schemes is quantified by the simulation results in Section V. Finally, we conclude in Section VI.

II. Relay-Assisted Single-Carrier–Frequency-Division Multiple-Access System Model

A. Transmitted Signal of Source MT

The relay-assisted SC-FDMA system considered supports K uplink users referred to as the source MTs in a cell. There

[1]PCEs are imposed on the MT's transmit power due to the feedback delay and estimation errors at the BS.

[2]Optimized transmit power sharing of cooperative MTs is assigned by the BS through feedback channel by ignoring the PCE.

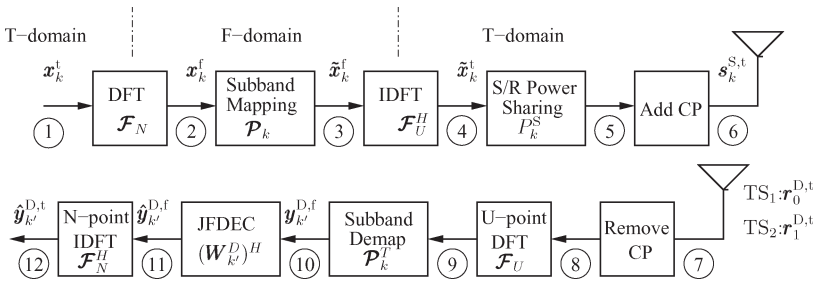

Fig. 1. DFT-S-OFDMA-style transmitter and MMSE-assisted JFDEC BS receiver.

are also idle terminals, which can be activated as the relays. The transmitter's block diagram is shown in the upper illustration of Fig. 1. The U-symbol baseband equivalent discrete-time signal transmitted by the kth source MT before inserting the *cyclic prefix* (CP) may be expressed as [25]

$$\boldsymbol{s}_k^{\mathrm{S,t}} = \sqrt{P_k^{\mathrm{S}}}\boldsymbol{\mathcal{F}}_U^H \boldsymbol{\mathcal{P}}_k \boldsymbol{\mathcal{F}}_N \boldsymbol{x}_k^{\mathrm{t}} \tag{1}$$

where the superscript $^{\mathrm{t}}$ refers to the TD signal, whereas $\boldsymbol{\mathcal{F}}_U$ and $\boldsymbol{\mathcal{F}}_N$ denote the normalized U- and N-point *fast Fourier transform* (FFT) matrices, respectively. Furthermore, $\boldsymbol{\mathcal{P}}_k$ represents the mapping of the kth user symbols to the most appropriate N subbands selected from the entire set of $U = M \times N$ subbands, where M is the bandwidth expansion factor. We refer to this operation as subband mapping. In the FDMA context considered, this subband mapping regime guarantees that the maximum number of orthogonal users supported is equal to the BW expansion factor, i.e., we have $K \leqslant M$, and the MU system operates at its full load when we have $K = M$. Moreover, the interleaved subband mapping mode in our system is defined as $\mathcal{P}_{k,(u,i)} = 1$ if $u = iM + k$; otherwise, $\mathcal{P}_{k,(u,i)} = 0$ $(0 < u < U-1, 0 < i < N-1)$, where $\mathcal{P}_{k,(u,n)}$ is the (u,n)th entry of $\boldsymbol{\mathcal{P}}_k$, and we have $u = 0, 1, \ldots, U-1$, $n = 0, 1, \ldots, N-1$. In addition, $\boldsymbol{x}_k^{\mathrm{t}}$ denotes the original N-symbol information packet of the kth user. Finally, P_k^{S} is the source MT's transmitted power determined by the power allocation and subjected to PCE, as discussed in Section II-B.

B. Channel Modeling and Assumptions

For simplicity, we assume that the source MTs, relays, and BS are all located in a line and the relays roam between the source and *destination*. Let us assume that the length of the *source–destination* (S–D) link is the reference distance in the propagation model with a *path-loss exponent* η [27]. Then, the *instantaneous path-loss* values of the *relay channels*, which are denoted by G_{SR} for the *source–relay* (S–R) and G_{RD} for the *relay–destination* (R–D), respectively, become the corresponding relaying gains, which incorporate the effects of the *average path loss* combined with shadowing. In particular, the average path losses of the S–R and R–D links are denoted by $\delta_{\mathrm{SR}}^{-\eta}$ and $\delta_{\mathrm{RD}}^{-\eta}$, respectively, where $\delta_{\mathrm{SR}} + \delta_{\mathrm{RD}} = 1$, and δ_{SR} and δ_{RD} are the distance normalized by the S–D distance. The shadowing component is characterized by the *log-normal* distribution associated with a *zero mean* and a *standard deviation* of σ_ξ, i.e., we have $\xi(dB) \sim \mathcal{N}(0, \sigma_\xi^2)$. Therefore, we can write $G_{\mathrm{SR}} = \xi_{\mathrm{SR}}\delta_{\mathrm{SR}}^{-\eta}$, $G_{\mathrm{RD}} = \xi_{\mathrm{RD}}\delta_{\mathrm{RD}}^{-\eta}$, whereas the shadowing effect at the S–D link is denoted by ξ_{SD} [42].

Note that, in a *small-scale* scenario, we assume that the systems experience *frequency-selective fading* associated with L paths. However, each subcarrier is assumed to experience flat fading. We assume that *perfect channel-state information* (CSI) is available for both the relays and BS, including the path loss, shadowing, and *fast fading*.

Furthermore, to guarantee fair comparison between the *cooperative* and *noncooperative* systems, the total signal power P of each user is normalized to *unity*. In particular, the source and relay MTs' transmit power assigned to the kth user are quantified as $P_k^{\mathrm{S}} = \epsilon_k^{\mathrm{S}}\alpha_k^{\mathrm{S}}P$ and $P_k^{\mathrm{R}} = \epsilon_k^{\mathrm{R}}\alpha_k^{\mathrm{R}}P$, respectively. The imperfect power control effects imposed on the transmitted power of the MTs can be evaluated by modeling it using the classic log-normal distributed PCE with a standard deviation of σ_ϵ (in decibels), i.e., $\epsilon(dB) \sim \mathcal{N}(0, \sigma_\epsilon^2)$ [36]. In addition, we quantify the *power constraints* of the source and relay as

$$\alpha_k^{\mathrm{S}} + \alpha_k^{\mathrm{R}} = 1 \tag{2}$$

where α_k^{S} and α_k^{R} represent the *power sharing* between the source and the relay. Note that, in the SSR topology, the relay simultaneously transmits all the K users' signals while obeying the power constraint given by

$$\alpha_{\mathrm{R}} = \sum_{k=0}^{K-1} \alpha_k^{\mathrm{R}} = 1. \tag{3}$$

C. Relaying Models

To separate multiple users in the FD and, hence, to avoid MUI, each source MT is assigned a *single relay* by the BS according to the OR mechanism, as detailed in Section IV. The block diagram of the AF relay model is shown in Fig. 2. We assume that the cooperation is *half duplex time division* based. Hence, during the *first time slot* (TS_1), all the K source MTs *broadcast* their messages represented by $\boldsymbol{s}_k^{\mathrm{S,t}}$, $(k = 0, 1, \ldots, K-1)$, which are received by both the relays and the BS through the S–R and S–D links, respectively. During the *second time slot* (TS_2), which is the *cooperation phase*, we consider both the SDR and SSR scenarios.

In the SDR system, the relays only forward the signals from the dedicated source MT to the BS through the R–D links, implying that a total of K relays are required for K source MTs. The signal received by the k'th relay $(k' = 0, 1, \ldots, K-1)$

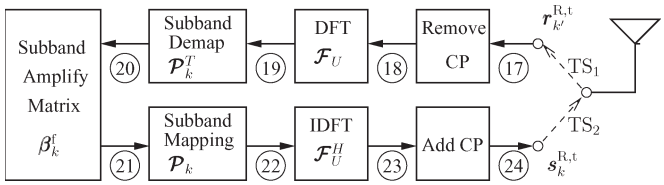

Fig. 2. AF relay structure.

and by the BS during TS_1 and TS_2, respectively, are expressed by the U-length vectors of

$$\boldsymbol{r}_{k'}^{\mathrm{R,t}} = \sqrt{G_{\mathrm{SR}}} \sum_{k=0}^{K-1} \tilde{\boldsymbol{H}}_k^{\mathrm{SR,t}} \boldsymbol{s}_k^{\mathrm{S,t}} + \tilde{\boldsymbol{n}}_k^{\mathrm{R,t}} \tag{4a}$$

$$\boldsymbol{r}_1^{\mathrm{D,t}} = \sqrt{G_{\mathrm{RD}}} \sum_{k'=0}^{K-1} \tilde{\boldsymbol{H}}_{k'}^{\mathrm{RD,t}} \boldsymbol{s}_{k'}^{\mathrm{R,t}} + \tilde{\boldsymbol{n}}_1^{\mathrm{D,t}} \tag{4b}$$

where $\tilde{\boldsymbol{H}}_k^{\mathrm{SR,t}}$ and $\tilde{\boldsymbol{H}}_{k'}^{\mathrm{RD,t}}$ host the $(U \times U)$ TD channel coefficient matrices of the S–R and R–D links for the kth and k'th source MT's signals, respectively, whereas $\tilde{\boldsymbol{n}}_k^{\mathrm{R,t}}$ and $\tilde{\boldsymbol{n}}_1^{\mathrm{D,t}}$ represent the U-length *complex-valued* additive white Gaussian noise (AWGN) vectors with a zero mean and a variance of σ_N^2 at each element, i.e., we have $\mathcal{CN}(0, \sigma_N^2)$ at both the kth *relay* and the BS, respectively.

Alternatively, a single relay may be shared by K source MTs to form a SSR uplink. Therefore, the representation of the signals received at the relay and the BS is given by

$$\boldsymbol{r}^{\mathrm{R,t}} = \sqrt{G_{\mathrm{SR}}} \sum_{k=0}^{K-1} \tilde{\boldsymbol{H}}_k^{\mathrm{SR,t}} \boldsymbol{s}_k^{\mathrm{S,t}} + \tilde{\boldsymbol{n}}_{\mathrm{R,t}} \tag{5a}$$

$$\boldsymbol{r}_1^{\mathrm{D,t}} = \sqrt{G_{\mathrm{RD}}} \tilde{\boldsymbol{H}}^{\mathrm{RD,t}} \boldsymbol{s}^{\mathrm{R,t}} + \tilde{\boldsymbol{n}}_1^{\mathrm{D,t}} \tag{5b}$$

where all the K source signals are embedded in the forwarded messages, which is denoted by $\boldsymbol{s}^{\mathrm{R,t}}$.

By invoking the subband-based equalization-aided AF scheme, the relay's received TD signals are first transformed to the FD by the U-point DFT operation and then demapped to the appropriate N subbands by $\boldsymbol{\mathcal{P}}_k^T$, which we refer to as *subband demapping* [24]. Each user's resulting signal is multiplied by the $(N \times N)$-element diagonal matrix as

$$\boldsymbol{\beta}_k^{\mathrm{f}} = \mathrm{diag}\left\{\beta_{k,0}^{\mathrm{f}}, \beta_{k,1}^{\mathrm{f}}, \ldots, \beta_{k,(N-1)}^{\mathrm{f}}\right\} \tag{6}$$

where the nth element is the specific *gain factor* of the nth subband, yielding [25]

$$\beta_{k,n}^{\mathrm{f}} = \sqrt{P_k^{\mathrm{R}} / \left[P_k^{\mathrm{S}} G_{\mathrm{SR}} \left|h_{k,n}^{\mathrm{SR,f}}\right|^2 + \sigma_N^2\right]}. \tag{7}$$

Then, the relay's signal that corresponds to the kth user is mapped to the subbands assigned to the kth source MT. We refer to the joint subband mapping and demapping procedure as the subband remapping operation. Therefore, the relay's transmission is free from interference, because neither the source MT nor the relay inflicts interference during relaying. Then, the U-point inverse discrete Fourier transform (IDFT) operation is invoked to transform the signal to the TD before it is transmitted to the BS. Finally, the transmitted signal of the kth relay during TS_2 is expressed as

$$\boldsymbol{s}_k^{\mathrm{R,t}} = \sqrt{P_k^{\mathrm{S}} G_{\mathrm{SR}}} \boldsymbol{\mathcal{F}}_U^H \boldsymbol{\mathcal{P}}_k \boldsymbol{\beta}_k^{\mathrm{f}} \boldsymbol{H}_k^{\mathrm{SR,f}} \boldsymbol{x}_k^{\mathrm{f}} + \bar{\boldsymbol{n}}_k^{\mathrm{R,t}} \tag{8}$$

where $\boldsymbol{H}_k^{\mathrm{SR,f}}$ represents the kth user's $(N \times N)$-element diagonal equivalent FD channel matrix that characterizes the S–R link, i.e., we have

$$\begin{aligned} \boldsymbol{H}_k^{\mathrm{SR,f}} &= \boldsymbol{\mathcal{P}}_k^T \boldsymbol{\mathcal{F}}_U \tilde{\boldsymbol{H}}_k^{\mathrm{SR,t}} \boldsymbol{\mathcal{F}}_U^H \boldsymbol{\mathcal{P}}_k \\ &= \mathrm{diag}\left\{h_{k,0}^{\mathrm{SR,f}}, h_{k,1}^{\mathrm{SR,f}}, \ldots, h_{k,(N-1)}^{\mathrm{SR,f}}\right\}. \end{aligned} \tag{9}$$

Note that the noise imposed on the kth user's signal is affected at the relay as

$$\tilde{\boldsymbol{n}}_k^{\mathrm{R,t}} = \boldsymbol{\mathcal{F}}_U^H \boldsymbol{\mathcal{P}}_k \boldsymbol{\beta}_k^{\mathrm{f}} \boldsymbol{\mathcal{P}}_k^T \boldsymbol{\mathcal{F}}_U \tilde{\boldsymbol{n}}_k^{\mathrm{R,t}} \tag{10}$$

where the noise imposed on the other users' subbands is removed as an additional benefit.

III. Signal Detection

A. Representation of Received Signal at the BS

The BS receiver structure is portrayed in Fig. 1, lower part. After removing the CP, the U-point DFT transforms the TD signal to the FD, followed by subband demapping at the BS receiver. Then, the FD signals of the kth user received through the direct branch during TS_1 and signals that arrive through the relaying branch during TS_2 can be expressed by the N-symbol vectors of

$$\boldsymbol{y}_{0,k'}^{\mathrm{D,f}} = \sqrt{P_{k'}^{\mathrm{S}} \xi_{\mathrm{SD}}} \boldsymbol{H}_{k'}^{\mathrm{SD,f}} \boldsymbol{x}_{k'}^{\mathrm{f}} + \boldsymbol{n}_0^{\mathrm{D,f}} \tag{11a}$$

$$\boldsymbol{y}_{1,k'}^{\mathrm{D,f}} = \sqrt{P_{k'}^{\mathrm{S}} G_{\mathrm{RD}} G_{\mathrm{SR}}} \boldsymbol{H}_{k'}^{\mathrm{RD,f}} \boldsymbol{\beta}_{k'}^{\mathrm{f}} \boldsymbol{H}_{k'}^{\mathrm{SR,f}} \boldsymbol{x}_{k'}^{\mathrm{f}} + \bar{\boldsymbol{n}}_1^{\mathrm{D,f}} \tag{11b}$$

where $\boldsymbol{H}_{k'}^{\mathrm{SD,f}}$ and $\boldsymbol{H}_{k'}^{\mathrm{RD,f}}$ are the $(N \times N)$-element equivalent diagonal FD channel matrices at the S–D and R–D links, respectively. Furthermore, $\boldsymbol{n}_0^{\mathrm{D,f}}$ and $\bar{\boldsymbol{n}}_1^{\mathrm{D,f}}$ represent the noise vectors with a length of N and represented by $\mathcal{CN}(0, \sigma_N^2)$, which are imposed at the BS during the two time slots, respectively. We amalgamate the aforementioned two equations into a $2N$-length joint observation vector as

$$\boldsymbol{y}_{k'}^{\mathrm{D,f}} = \sqrt{P_{k'}^{\mathrm{S}}} \boldsymbol{H}_{k'}^{\mathrm{D,f}} \boldsymbol{x}_{k'}^{\mathrm{f}} + \boldsymbol{n}^{\mathrm{D,f}} \tag{12}$$

where the $(2N \times N)$-element joint equivalent FD channel matrix is given by

$$\boldsymbol{H}_{k'}^{\mathrm{D,f}} = \begin{bmatrix} \boldsymbol{H}_{0,k'}^{\mathrm{D,f}} \\ \boldsymbol{H}_{1,k'}^{\mathrm{D,f}} \end{bmatrix} = \begin{bmatrix} \sqrt{\xi_{\mathrm{SD}}} \boldsymbol{H}_{k'}^{\mathrm{SD,f}} \\ \sqrt{G_{\mathrm{RD}} G_{\mathrm{SR}}} \boldsymbol{H}_{k'}^{\mathrm{RD,f}} \boldsymbol{\beta}_{k'}^{\mathrm{f}} \boldsymbol{H}_{k'}^{\mathrm{SR,f}} \end{bmatrix}. \tag{13}$$

In addition, we formulate the nth element of the diagonal matrices $\boldsymbol{H}_{0,k'}^{\mathrm{D,f}}$ and $\boldsymbol{H}_{1,k'}^{\mathrm{D,f}}$ as

$$h_{0,k',n}^{\mathrm{D,f}} = \sqrt{\xi_{\mathrm{SD}}} h_{SD,k'n}^{\mathrm{f}} \tag{14a}$$

$$h_{1,k',n}^{\mathrm{D,f}} = \beta_{k',n}^{\mathrm{f}} \sqrt{G_{\mathrm{RD}} G_{\mathrm{SR}}} h_{k',n}^{\mathrm{RD,f}} h_{k',n}^{\mathrm{SR,f}}. \tag{14b}$$

Similarly, the total received noise of the k'th user at the BS includes the noise contribution imposed by the k'th relay after the aforementioned subband remapping operation plus the noise added at the BS during the two time slots, which is expressed by a $2N$-length vector as

$$\boldsymbol{n}^{\mathrm{D,f}} = \begin{bmatrix} \boldsymbol{n}_0^{\mathrm{D,f}} \\ \bar{\boldsymbol{n}}_1^{\mathrm{D,f}} \end{bmatrix} = \begin{bmatrix} \boldsymbol{\mathcal{P}}_{k'}^T \boldsymbol{\mathcal{F}}_U \tilde{\boldsymbol{n}}_0^{\mathrm{D,t}} \\ \boldsymbol{\mathcal{P}}_{k'}^T \boldsymbol{\mathcal{F}}_U \left(\sqrt{G_{\mathrm{RD}}} \tilde{\boldsymbol{H}}_{k'}^{\mathrm{RD,t}} \bar{\boldsymbol{n}}_{k'}^{\mathrm{R,t}} + \tilde{\boldsymbol{n}}_1^{\mathrm{D,t}} \right) \end{bmatrix}. \tag{15}$$

B. MMSE-Assisted JFDEC

Based on (12), it can readily be shown that the *optimum* MMSE solution is given by

$$\boldsymbol{W}_{k'}^{\mathrm{D}} = \left(\boldsymbol{R}_{k'}^{\mathrm{yD}} \right)^{-1} \boldsymbol{R}_{k'}^{\mathrm{yxD}} \tag{16}$$

where the *autocorrelation* matrix of $\boldsymbol{y}_{k'}^{\mathrm{D,f}}$ is given by

$$\boldsymbol{R}_{k'}^{\mathrm{yD}} = P_{k'}^{\mathrm{S}} \boldsymbol{H}_{k'}^{\mathrm{D,f}} \left(\boldsymbol{H}_{k'}^{\mathrm{D,f}} \right)^H + \boldsymbol{R}_{\mathrm{nD}} \tag{17}$$

with $\boldsymbol{R}_{\mathrm{nD}} = \mathrm{E}[\boldsymbol{n}^{\mathrm{D,f}} (\boldsymbol{n}^{\mathrm{D,f}})^H] = \mathrm{diag}\{\boldsymbol{R}_0^{\mathrm{nD}}, \boldsymbol{R}_1^{\mathrm{nD}}\}$ denoting the *covariance* matrix of $\boldsymbol{n}^{\mathrm{D,f}}$, where $\boldsymbol{R}_0^{\mathrm{nD}} = \mathrm{E}[\boldsymbol{n}_0^{\mathrm{D,f}} (\boldsymbol{n}_0^{\mathrm{D,f}})^H] = \sigma_N^2 \boldsymbol{I}_N$ and $\boldsymbol{R}_1^{\mathrm{nD}} = \mathrm{E}[\bar{\boldsymbol{n}}_1^{\mathrm{D,f}} (\bar{\boldsymbol{n}}_1^{\mathrm{D,f}})^H] = \sigma_N^2 [G_{\mathrm{RD}} \boldsymbol{H}_{k'}^{\mathrm{RD,f}} \boldsymbol{\beta}_{k'}^{\mathrm{f}} (\boldsymbol{\beta}_{k'}^{\mathrm{f}})^H (\boldsymbol{H}_{k'}^{\mathrm{RD,f}})^H + \boldsymbol{I}_N]$. Thus, the corresponding power of the noise components $\boldsymbol{n}_0^{\mathrm{D,f}}$ and $\bar{\boldsymbol{n}}_1^{\mathrm{D,f}}$ in the nth subband during TS_1 and TS_2 can be expressed as $\mathcal{N}_{0,n}^{\mathrm{D}} = \sigma_N^2$ and $\mathcal{N}_{1,n}^{\mathrm{D}} = \sigma_N^2 (\beta_{k',n}^{\mathrm{f}})^2 G_{\mathrm{RD}} |h_{k',n}^{\mathrm{RD,f}}|^2 + \sigma_N^2$, respectively. In (16), $\boldsymbol{R}_{k'}^{\mathrm{yxD}}$ is the *cross-correlation* matrix between $\boldsymbol{y}_{k'}^{\mathrm{D,f}}$ and $\boldsymbol{x}_{S,k'}^{\mathrm{f}}$, which can be expressed as

$$\boldsymbol{R}_{k'}^{\mathrm{yxD}} = P_{k'}^{\mathrm{S}} \boldsymbol{H}_{k'}^{\mathrm{D,f}}. \tag{18}$$

Therefore, when substituting (17) and (18) into (16), the $(2N \times N)$-element *optimum-weight* matrix of the MMSE-aided JFDEC is formulated as

$$\boldsymbol{W}_{k'}^{\mathrm{D}} = P_{k'}^{\mathrm{S}} \left[P_{k'}^{\mathrm{S}} \boldsymbol{H}_{k'}^{\mathrm{D,f}} \left(\boldsymbol{H}_{k'}^{\mathrm{D,f}} \right)^H + \boldsymbol{R}_{\mathrm{nD}} \right]^{-1} \boldsymbol{H}_{k'}^{\mathrm{D,f}} \tag{19a}$$

where the matrix inversion operation can be applied to the $(N \times N)$-element diagonal matrices $\boldsymbol{R}_0^{\mathrm{nD}}$ and $\boldsymbol{R}_1^{\mathrm{nD}}$, respectively. Note that $\boldsymbol{R}_{k'}^{\mathrm{yD}}$ is a $(2N \times 2N)$-element nondiagonal matrix. Hence, the complexity of inverting $\boldsymbol{R}_{k'}^{\mathrm{yD}}$ might be high. To jointly implement the low-complexity single-tap FDE and diversity combining, the *matrix inversion lemma*[3] of [24] can be invoked, and then, (19a) is formulated as

$$\boldsymbol{W}_{k'}^{\mathrm{D}} = P_{k'}^{\mathrm{S}} \boldsymbol{R}_{\mathrm{nD}}^{-1} \boldsymbol{H}_{k'}^{\mathrm{D,f}} \left[P_{k'}^{\mathrm{S}} \left(\boldsymbol{H}_{k'}^{\mathrm{D,f}} \right)^H \boldsymbol{R}_{\mathrm{nD}}^{-1} \boldsymbol{H}_{k'}^{\mathrm{D,f}} + \boldsymbol{I}_N \right]^{-1}. \tag{19b}$$

Consequently, by substituting $\boldsymbol{H}_{k'}^{\mathrm{D,f}}$ and $\boldsymbol{R}_{\mathrm{nD}}$ into the aforementioned equation, we obtain $\boldsymbol{W}_{k'}^{\mathrm{D}}$, which is constituted by two $(N \times N)$-element diagonal matrices, yielding

$$\boldsymbol{W}_{k'}^{\mathrm{D}} = \begin{bmatrix} \left(\boldsymbol{R}_0^{\mathrm{nD}} \right)^{-1} \boldsymbol{H}_{0,k'}^{\mathrm{D,f}} \\ \left(\boldsymbol{R}_1^{\mathrm{nD}} \right)^{-1} \boldsymbol{H}_{1,k'}^{\mathrm{D,f}} \end{bmatrix} \left[\left(\boldsymbol{H}_{0,k'}^{\mathrm{D,f}} \right)^H \left(\boldsymbol{R}_0^{\mathrm{nD}} \right)^{-1} \boldsymbol{H}_{0,k'}^{\mathrm{D,f}} + \left(\boldsymbol{H}_{1,k'}^{\mathrm{D,f}} \right)^H \left(\boldsymbol{R}_1^{\mathrm{nD}} \right)^{-1} \boldsymbol{H}_{1,k'}^{\mathrm{D,f}} + 1/P_{k'}^{\mathrm{R}} \boldsymbol{I}_N \right]^{-1}. \tag{19c}$$

Hence, the nth and $(n+N)$th elements of $\boldsymbol{W}_{k'}^{\mathrm{D}}$ can be expressed by

$$w_{k',n}^{\mathrm{D}} = h_{0,k',n}^{\mathrm{D,f}} e_{k'n} / \sigma_N^2 \quad w_{k',(n+N)}^{\mathrm{D}} = h_{1,k',n}^{\mathrm{D,f}} e_{k'n} / \mathcal{N}_{1,n}^{\mathrm{D}} \tag{20}$$

where $e_{k'n}$ is given by

$$e_{k'n} = \left(\left| h_{0,k',n}^{\mathrm{D,f}} \right|^2 / \sigma_N^2 + \left| h_{1,k',n}^{\mathrm{D,f}} \right|^2 / \mathcal{N}_{1,n}^{\mathrm{D}} + 1/P_{k'}^{\mathrm{R}} \right)^{-1}. \tag{21}$$

In fact, $e_{k'n}$ is the FD MMSE value in the nth subband of the k'th user's signal, which will be discussed in more detail in Section III-C. It will be shown that the weight matrix $\boldsymbol{W}_{k'}^{\mathrm{D}}$ can jointly carry out single-tap FDE and diversity combining of the direct and relay branches. In particular, the coefficients $h_{0,k',n}^{\mathrm{D,f}} e_{k'n}$ and $h_{1,k',n}^{\mathrm{D,f}} e_{k'n}$ in (20) are used for single-tap FDE in conjunction with diversity combining while obeying the MMSE criterion, where noise whitening is carried out at both branches by normalizing it according to the noise power σ_N^2 and $\mathcal{N}_{1,n}^{\mathrm{D}}$, respectively.

C. Relationships of MMSE, SNR, and SINR

Correspondingly, upon applying the weight matrix $(\boldsymbol{W}_{k'}^{\mathrm{D}})^H$ to $\boldsymbol{y}_{k'}^{\mathrm{D,f}}$, signals that arrive from both the direct and relaying branches are combined into an N-length observation vector in the FD, which are then transformed into the TD decision variable vector for $\boldsymbol{x}_{k'}^{\mathrm{t}}$ by the N-point IDFT, yielding

$$\hat{\boldsymbol{y}}_{k'}^{\mathrm{D,t}} = \boldsymbol{\mathcal{F}}_N^H \left(\boldsymbol{W}_{k'}^{\mathrm{D}} \right)^H \boldsymbol{y}_{k'}^{\mathrm{D,f}} = \boldsymbol{A}_{k'}^{\mathrm{t}} \boldsymbol{x}_{k'}^{\mathrm{t}} + \hat{\boldsymbol{n}}_D^{\mathrm{t}} \tag{22}$$

where $\boldsymbol{A}_{k'}^{\mathrm{t}}$ is the $(N \times N)$-element TD circulant influence matrix of desired signals, and $\hat{\boldsymbol{n}}_D^{\mathrm{t}}$ is the N-length TD noise vector after equalization. The gain factor between $\boldsymbol{x}_{k'}^{\mathrm{t}}$ and its estimate of $\hat{\boldsymbol{y}}_{k'}^{\mathrm{D,t}}$ is given by the diagonal elements of the matrix $\boldsymbol{A}_{k'}^{\mathrm{t}}$ [43].

Furthermore, the TD estimation error vector $\boldsymbol{e}_{k'}^{\mathrm{t}}$ between the transmitted signal $\boldsymbol{x}_{k'}^{\mathrm{t}}$ and the estimated signal $\hat{\boldsymbol{y}}_{k'}^{\mathrm{D,t}}$ can be expressed as

$$\boldsymbol{e}_{k'}^{\mathrm{t}} = \boldsymbol{x}_{k'}^{\mathrm{t}} - \hat{\boldsymbol{y}}_{k'}^{\mathrm{D,t}} = \boldsymbol{x}_{k'}^{\mathrm{t}} - \boldsymbol{A}_{k'}^{\mathrm{t}} \boldsymbol{x}_{k'}^{\mathrm{t}} - \hat{\boldsymbol{n}}_D^{\mathrm{t}} \tag{23}$$

where the covariance matrix of $\boldsymbol{e}_{k'}^{\mathrm{t}}$ is given by

$$\begin{aligned} \boldsymbol{R}_{e_{k'}^{\mathrm{t}}} &= \mathrm{E}\left[\boldsymbol{e}_{k'}^{\mathrm{t}} \left(\boldsymbol{e}_{k'}^{\mathrm{t}} \right)^H \right] \\ &= P \left[\boldsymbol{I}_N - 2\Re\left\{ A_{k'}^{\mathrm{t}} \right\} + \boldsymbol{A}_{k'}^{\mathrm{t}} \left(\boldsymbol{A}_{k'}^{\mathrm{t}} \right)^H \right] + \sigma_N^2 \boldsymbol{I}_N \end{aligned} \tag{24}$$

with $\Re\{\boldsymbol{A}_{k'}^{\mathrm{t}}\}$ denoting the real part of $\boldsymbol{A}_{k'}^{\mathrm{t}}$. Therefore, $\boldsymbol{R}_{e_{k'}^{\mathrm{t}}}$ is also an $(N \times N)$-element circulant matrix with identical diagonal elements, which implies that, due to the averaging effects

[3]Assuming that the matrices $\boldsymbol{A}$ and $\boldsymbol{B}$ have $(N \times N)$ and $(N \times M)$ elements, respectively, and $\boldsymbol{I}_M$ is an $(M \times M)$-element identity matrix, we have $(\boldsymbol{A} + \boldsymbol{B}\boldsymbol{B}^H)^{-1} \boldsymbol{B} = \boldsymbol{A}^{-1} \boldsymbol{B} (\boldsymbol{B}^H \boldsymbol{A}^{-1} \boldsymbol{B} + \boldsymbol{I}_M)^{-1}$.

of the N-point IDFT operation, all the kth users' resulting TD symbols within the vector have the same MMSE value $e_{k'}$. This MMSE value can be calculated as the average of the FD MMSE values over N subbands, yielding the MMSE of the joint solution as

$$e_{k'} = \frac{1}{N}\sum_{n=0}^{N-1} e_{k',n} = \frac{1}{N}\mathrm{Tr}\left[\boldsymbol{R}_{e^{\mathrm{f}}_{k'}}\right]. \tag{25}$$

Hence, (21) can be also derived by

$$\begin{aligned} e_{k',n} &= \left[\boldsymbol{R}_{e^{\mathrm{f}}_{k'}}\right]_n = \left[P^{\mathrm{S}}_{k'}\boldsymbol{I}_N - \left(\boldsymbol{R}^{\mathrm{yxD}}_{k'}\right)^H \boldsymbol{W}^{\mathrm{D}}_{k'}\right]_n \\ &= P^{\mathrm{S}}_{k'}/\left(\gamma^{\mathrm{D0}}_{k',n} + \gamma^{\mathrm{D1}}_{k',n} + 1\right) \end{aligned} \tag{26}$$

where the instantaneous received SNRs of the direct and relaying branches in the nth subband are expressed as

$$\gamma^{\mathrm{D0}}_{k',n} = \gamma^{\mathrm{SD}}_{k',n} = P^{\mathrm{S}}_{k'}\xi_{\mathrm{SD}}\left|h^{\mathrm{f}}_{SD,k'n}\right|^2/\sigma^2_N \tag{27a}$$

$$\gamma^{\mathrm{D1}}_{k',n} = \left(1/\gamma^{\mathrm{SR}}_{k',n} + 1/\gamma^{\mathrm{RD}}_{k',n}\right)^{-1} \tag{27b}$$

$$\gamma^{\mathrm{SR}}_{k',n} = P^{\mathrm{S}}_{k'}G_{\mathrm{SR}}\left|h^{\mathrm{SR,f}}_{k',n}\right|^2/\sigma^2_N \tag{27c}$$

$$\gamma^{\mathrm{RD}}_{k',n} = \frac{P^{\mathrm{R}}_{k'}G_{\mathrm{RD}}G_{\mathrm{SR}}\left|h^{\mathrm{RD,f}}_{k',n}\right|^2\left|h^{\mathrm{SR,f}}_{k',n}\right|^2}{\sigma^2_N\left(G_{\mathrm{SR}}\left|h^{\mathrm{SR,f}}_{k',n}\right|^2 + \sigma^2_N/P^{\mathrm{S}}_{k'}\right)}. \tag{27d}$$

We note that $e_{k',n}$ has already appeared in (21) and it is also equivalent to the general result for the optimum MMSE solution of the noncooperative scenario [24], [44].

Consequently, according to the relationship between the SINR and MMSE as a general feature of the MMSE criterion [24], we obtain the k'th user's instantaneous overall received SINR at the output of our proposed scheme in the form of

$$\begin{aligned} \gamma_{k'} &= P^{\mathrm{S}}_{k'}e^{-1}_{k'} - 1 \\ &= \left\{\frac{1}{N}\sum_{n=0}^{N-1}\left[\begin{array}{c} 1+\gamma^{\mathrm{SD}}_{k',n}+ \\ \left(1/\gamma^{\mathrm{SR}}_{k',n} + 1/\gamma^{\mathrm{RD}}_{k',n}\right)^{-1}\end{array}\right]^{-1}\right\}^{-1} - 1 \end{aligned} \tag{28}$$

which is derived in the Appendix in the form of (45).

D. Energy Consumption Metrics

To evaluate the MU system's performance in terms of the achievable power reduction, we introduce the following two energy consumption metrics: 1) the energy consumption rate (ECR), which is expressed in the unit of joules per bit, and 2) the ECG, which is defined as the ratio of the ECR of reference system over the ratio of the system advocated [41]. Therefore, the ECR of single-hop direct transmission that operates without cooperation may be defined as

$$ECR_{\mathrm{dir}} = \sum_{k=0}^{K-1}\frac{P_kT}{R^{\mathrm{dir}}_kT} = \sum_{k=0}^{K-1}\frac{P_k}{R^{\mathrm{dir}}_k} = \frac{KP}{R^{\mathrm{dir}}_\Sigma} \tag{29}$$

where T denotes the time-slot duration, i.e., time duration per hop, whereas $R^{(\cdot)}_kR^{(\cdot)}_\Sigma$ denote the achievable ergodic single-user rate and MU sum rates of the $(\cdot)$-type transmission, i.e., of direct or AF-cooperative transmissions.

Similarly, the ECR of two-hop AF-cooperative transmissions may be expressed as

$$ECR_{\mathrm{AF}} = \sum_{k=0}^{K-1}\frac{P^{\mathrm{S}}_kT + P^{\mathrm{R}}_kT}{R^{\mathrm{AF}}_k2T} = \sum_{k=0}^{K-1}\frac{P^{\mathrm{S}}_k + P^{\mathrm{R}}_k}{2R^{\mathrm{AF}}_k}. \tag{30}$$

Because we assume $\sum_{k=0}^{K-1}(P^{\mathrm{S}}_k + P^{\mathrm{R}}_k) = KP$, by using the direct transmission as a reference, the ECG of cooperative transmissions is given by

$$ECG = \frac{ECR_{\mathrm{dir}}}{ECR_{\mathrm{AF}}} = \frac{2R^{\mathrm{AF}}_\Sigma}{R^{\mathrm{dir}}_\Sigma}. \tag{31}$$

We assume that the system bandwidth was normalized to unity in our baseband processing; hence, $R^{(\cdot)}_\Sigma$, expressed in terms of bits per second per hertz, is given by

$$R^{(\cdot)}_\Sigma = \mathrm{E}\left[\sum_{k=0}^{K-1}\frac{1}{N_{\mathrm{TS}}}\log_2\left(1+\gamma^{(\cdot)}_k\right)\right] \tag{32}$$

where the factor $1/N_{\mathrm{TS}}$ indicates the effect of the N_{TS} time slots required for direct or cooperative transmission.

Therefore, the corresponding instantaneous SINR of the kth user may be expressed as

$$\gamma^{(\cdot)}_k = \left[\frac{1}{N}\sum_{n=0}^{N-1}\left(1+\gamma^{(\cdot)}_{k,n}\right)^{-1}\right]^{-1} - 1. \tag{33}$$

In particular, for direct transmission, we have an equivalent instantaneous SNR in the nth subband of the kth user given by

$$\gamma^{\mathrm{dir}}_{k,n} = P_k\xi_{\mathrm{dir}}\left|h^{\mathrm{dir,f}}_{k,n}\right|^2\Big/\sigma^2_N. \tag{34}$$

By contrast, for AF cooperation, the kth user's received equivalent instantaneous SNR in the nth subband can be expressed, according to (28), as

$$\gamma^{\mathrm{AF}}_{k,n} = \gamma^{\mathrm{SD}}_{k,n} + \left[\left(\gamma^{\mathrm{SR}}_{k,n}\right)^{-1} + \left(\gamma^{\mathrm{RD}}_{k,n}\right)^{-1}\right]^{-1}. \tag{35}$$

IV. Opportunistic Cooperative Relaying

OR allows a single relay to be selected from a cluster of $J(J>0)$ inactive MTs, which are the RCs, depending on which MT provides the best *end-to-end* link between the source and the destination [12]. In this section, the source/relay power sharing and relay selection are investigated for power-efficient opportunistic cooperation. Three relay selection schemes—the SU-RS, MU-RS, and MA-RS regimes—are shown in Fig. 3. The BS is assumed to acquire the channel-state information at receiver (CSIR) and the SNR of all the cooperative links based on pilot-assisted channel estimation, which were formulated in (27a), (27c), and (27d). Power sharing and relay selection

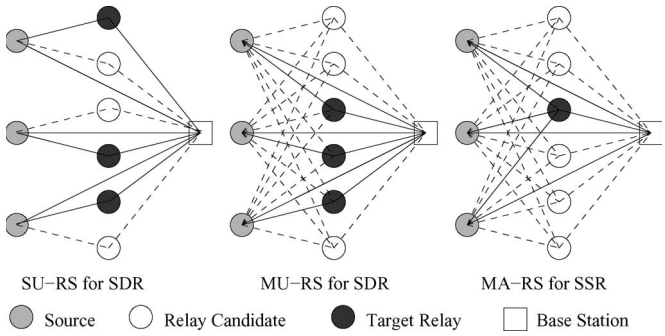

Fig. 3. Opportunistic cooperative-relaying-aided SC-FDMA uplink.

are carried out with the objective of maximizing the average received instantaneous SINR of each user at the BS for both the direct and relaying branches. In addition, we assume that the transmissions of the S–D, S–R, and R–D links are orthogonal, and hence, they do not impose an increased MUI.

A. Source/Relay Power Allocation

The proposed systems invoke the linear and adaptive source/relay power sharing modes. The family of linear power sharing includes *equal power allocation* (EPA) and *default power allocation* (DPA) for the SDR and SSR systems, respectively. In particular, the EPA mode adjusts the transmitted powers of the kth source and jth RC to be equal, whereas the DPA mode shares the transmitted power between the source MT and relay according to the number of active source users within the system. Hence, we have

$$\text{EPA for SDR:} \quad \alpha_{j,k}^{\mathrm{S}} = \alpha_{j,k}^{\mathrm{R}} = 0.5 \tag{36a}$$

$$\text{DPA for SSR:} \quad \alpha_{j,k}^{\mathrm{S}} = 1 - 1/K$$
$$\alpha_{j,k}^{\mathrm{R}} = 1/K. \tag{36b}$$

Alternatively, the adaptive OPA mode may be invoked for both SDR and SSR systems, which maximizes the average SINR expression of (28) for the kth user with the aid of the jth RC by associating the CSIR, yielding

$$\begin{aligned} \max_{\alpha_{j,k}^{\mathrm{S}}, \alpha_{j,k}^{\mathrm{R}}} \quad & \gamma_{j,k}^{\mathrm{AF}} \left(\alpha_{j,k}^{\mathrm{S}}, \alpha_{j,k}^{\mathrm{R}}\right) \\ \text{subject to} \quad & \alpha_{j,k}^{\mathrm{S}} + \alpha_{j,k}^{\mathrm{R}} = 1 \\ & \alpha_{j,k}^{\mathrm{S}} > 0 \quad \alpha_{j,k}^{\mathrm{R}} > 0 \\ & \text{for SSR:} \sum_{k=0}^{K-1} \alpha_{j,k}^{\mathrm{R}} = 1. \end{aligned} \tag{37}$$

B. SU-RS

Initially, we examine the relay selection schemes designed for the SDR topology. If the total number of idle MTs that access the single-cell BS is high, more RCs may be considered for activation as the target relay. Because each source MT can seek a target relay from a cluster of J RCs, which are independent of the other source MT's RC, we propose the SU-RS scheme, where a total of $(K \times J)$ inactive MTs are required to support K source MTs. The BS calculates the overall SINR of the kth user while tentatively relying on any of the J RCs and then selects the RC with the maximum SINR, which is associated with the index of j_k^{opt}, as formulated in

$$j_k^{\mathrm{opt}} = \arg \max_{j \in [0, J-1]} \left\{ \gamma_{j,k}^{\mathrm{AF}} \right\} \quad (J > 0). \tag{38}$$

C. MU-RS

However, when the total number of inactive MTs that roam within a cell is low, the number of available RCs may become insufficient, because $J \times K$ RCs would be required for K sources in SU-RS. To circumvent this limitation of the SDR regime, we propose the MU-RS scheme, which allows the multiple-source users to access a shared RC, where each source's data are forwarded by selecting a single desired relay for cooperative transmission. In particular, a cluster of K source MTs is collectively associated with a cluster of $J(J \geq K)$ RCs, but the system only requires a total of K target relays. Furthermore, the system invokes the *optimal partner ordering* method by extending the *relay-ordering* regime in [16] to take into account both multiple sources and multiple relays to optimize *cooperative partner pairing*. Our regime calculates the overall SINR of all the K source MTs' signal by tentatively assuming cooperation with all the J RCs and chooses the specific source–relay pairs with the highest K received SINR values at the BS, which are provided by the RCs that correspond to the particular source MTs. In particular, at the ith iteration, the desired relay's index $j_{k,i}^{\mathrm{opt}}$ selected for assisting the kth source MT is assumed to be the pairing index i, which are compiled in *descending order*, yielding

$$j_{k,i}^{\mathrm{opt}} = \arg \max_{j \in [0, J-1], k \in [0, K-1]} \left\{ \gamma_{j,k}^{\mathrm{AF}} \right\} \quad (J \geq K). \tag{39}$$

Thus, upon removing the kth source MT and the $j_{k,i}^{\mathrm{opt}}$th relay from the selected pools, the target relay of the $(k+1)$th user may be allocated during the next iteration using (39).

D. MA-RS

By contrast, in the SSR system, the relay selection should take into account the overall performance of all the links from all source MTs that aim at sharing a relay, because multiple-source MTs have to gain access to a common target relay by evaluating the benefits of an entire cluster of RCs, where the minimum number of RCs is independent of the number of sources, i.e., we have $J > 0$. Hence, the proposed MA-RS scheme looks for a single relay indicated by j^{opt}, which offers the maximum sum of SINRs results for the K-source MTs, which is formulated as

$$j^{\mathrm{opt}} = \arg \max_{j \in [0, J-1]} \left\{ \gamma_{j,\Sigma} = \sum_{k=0}^{K-1} \gamma_{j,k}^{\mathrm{AF}} \right\} \quad (J > 0). \tag{40}$$

E. Computational Complexity

The computational complexity of the different power allocation and relay selection procedures should be quantified

TABLE I
SIMULATION PARAMETERS

Subband mapping scheme	Interleaved
Number of source users	$K = 4, 8$
Total number of relay candiates	16 or varying
Number of subbands per user	$N = 8$
Bandwidth expansion factor	$M = 8$
Total number of subbands	$U = 64$
Number of paths	$L = 8$
Path-loss exponent	$\eta = 0, 4$
Shadowing variance	$\sigma_\xi^2 = 0, 2, 4, 8$ (dB)
PCE variance	$\sigma_\epsilon^2 = 0, 2$ (dB)

to find the most suitable algorithm. The EPA benefits from the lowest complexity, regardless of the number of users and relays involved, whereas the DPA requires both the sources and the relays to have the knowledge of K, but beneficially, it dispenses with any iterations. The OPA exhibits the highest complexity, which depends on both the specific optimization algorithm employed and the stepsize of the power control strategy adopted. From a MU point of view, SU-RS, MU-RS, and MA-RS all require $(K \times J)$ iterations among RCs for all K users. However, from a SU point of view, SU-RS only needs J iterations, which is independent of the number of sources, whereas MU-RS still requires $(K \times J)$ iterations to calculate the index of the desired relay for each source MT. In addition, RRS does not require any iteration among RCs. We assume that, in practical cellular systems, the number of cooperative users and the number of RCs within each cluster may not be high, e.g., less than ten in total, but lower complexity search algorithms may be considered for this selection stage to reduce the signal processing power and time delay.

V. SIMULATION RESULTS AND DISCUSSIONS

In our simulations, we investigate the uncoded binary phase-shift keying (BPSK) modulated link-level performance of the proposed schemes subject to shadowing under imperfect power control with propagation path-loss scenario, experiencing the frequency-selective Rayleigh fading. Our parameters are summarized in Table I.

Initially, we consider a simple idealized system that experiences only small-scale fading, whereas the effects of shadowing, path-loss, relay selection, and power control are all ignored. Fig. 4 illustrates the *bit error ratio* (BER) versus the E_b/N_0 performance of the AF relaying system that relies on different receiver solutions for *full-load* uplink transmissions over a dispersive channel with $L = 8$ paths while supporting $K = 8$ users. Compared to the FDE-EGC method, the proposed JFDEC scheme jointly carries out FDE and diversity combining through the optimized weights of (20) over each subband for both the direct and relaying branches. Quantitatively, our proposed scheme can achieve approximately 4-dB power reduction at a BER of 10^{-4}, which is an explicit benefit of the cooperative diversity gain, whereas the FDE-EGC scheme only saves 2-dB power.

Furthermore, to characterize the effects of varying the ratio of the source/relay power and the locations of the relays in the presence of path loss but without shadowing, Fig. 5 depicts the

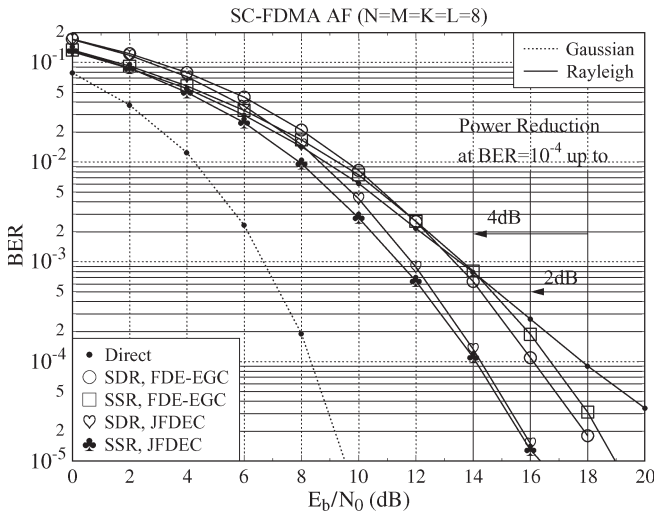

Fig. 4. BER performance comparison and power reduction by ignoring the effects of path and shadowing.

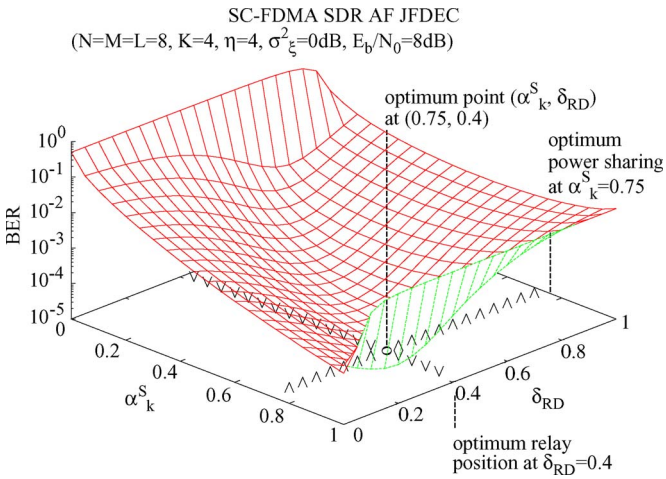

Fig. 5. Effects of varying shared power and relaying distance.

BER versus the $(\alpha_k^{\mathrm{S}}, \delta_{\mathrm{RD}})$ performance of the SDR topology for $\eta = 4$ at $E_b/N_0 = 8$ dB, where perfect power control is assumed for both the source and the relay. Because the path loss of the S–R and R–D links is lower than the path loss of the S–D link, high relaying gains are attainable at the BS through the relaying branch, which is confirmed by the curve denoted by the $\vee$ marker. Because we assume that the total transmitted power of the system is constant, the source MT can transmit its own signal at a higher α_k^{S}, as indicated by the curve marked by $\wedge$ for $\alpha_k^{\mathrm{S}} = 0.75$, which is then attenuated by the long-distance S–D and S–R links during TS_1. By contrast, the relay transmits the signal forwarded to the destination at a lower α_k^{R} in TS_2 when the relay roams within the desired relaying area near the BS, as indicated by the curve marked by legend $\vee$ for $\delta_{\mathrm{RD}} = 0.4$, which is expected to have a high relaying gain. Therefore, observing the relay located at this optimum position, the BER performance of the EPA mode recorded for $\alpha_k^{\mathrm{S}} = 0.5$ only slightly decreases compared with the OPA mode for $\alpha_k^{\mathrm{S}} = 0.75$ but requires lower complexity. In addition, due to the power constraint of the SSR uplink, the default transmit power of the source MT is a function of K. Hence, the optimum

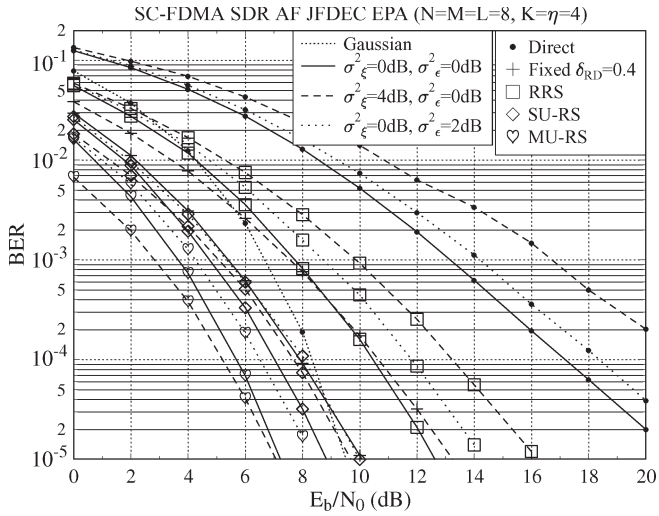

Fig. 6. SDR: BER performance of relay selection schemes that invoke EPA.

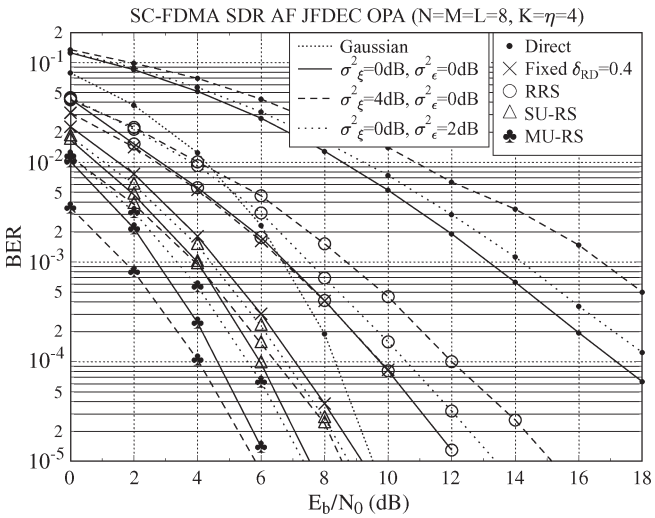

Fig. 7. SDR: BER performance of relay selection schemes that invoke OPA.

value of α_k^{S} may be the α_k^{S} of DPA for the SSR topology, which is larger than the optimum value of α_k^{S} designed for the SDR topology. In summary, both EPA and DPA are more practical schemes when subjected to imperfect power control, which is an explicit benefit of their low complexity, when invoked in the context of the SDR and SSR topologies, respectively. By contrast, OPA improves the achievable performance at an increased complexity.

For fair comparison, we assume that we have $K = 4$ source MTs, assisted by $J = 4$ and $J = 16$ RCs for SU-RS and MU-RS, respectively. Upon varying the effects of shadowing under imperfect power control at all links for transmission over Rayleigh fading channels in the presence of path loss for $\eta = 4$, Figs. 6 and 7 characterize the overall average BER versus the E_b/N_0 performance of different relay-selection-aided AF systems that invoke EPA and OPA, respectively. As observed in Fig. 7, the achievable gain of the OPA recorded for $\alpha_k^{\mathrm{S}} = 0.75$ is limited to about 1 dB at a BER of 10^{-4} compared to the EPA curves recorded for $\alpha_k^{\mathrm{S}} = 0.5$ in Fig. 6, which indicates the robustness of the proposed cooperative regime. In addition, we know that, according to Fig. 5, the activation of the relay in the vicinity of the optimal location can achieve a similar performance to OPA. Compared with the RRS characterized in both Figs. 6 and 7, the fixed relay associated with the optimal relay position of $\delta_{\mathrm{RD}} = 0.4$ offers a 3-dB relaying gain at a BER of 10^{-4}, whereas both SU-RS and MU-RS provide a substantial MU diversity gain, which is about 4 dB at a BER of 10^{-4}. Furthermore, the proposed MU-RS has the edge over SU-RS, providing an additional MU diversity gain in excess of 2 dB, which is a benefit of the relay selection procedure that avoids the effects of deep shadow fading. As a result, the transmitted power can be reduced by about $(E_b/N_0)_\Delta = 4$ dB at a BER of 10^{-4} when we have $\sigma_\xi^2 = 4$ dB, $\sigma_\epsilon^2 = 0$ dB.

By contrast, the relay selection effects on the attainable BER performance of the SSR system upon varying the shadow-fading variance under imperfect power control are characterized in Fig. 8. The fixed relay can obtain a 3-dB relaying gain, which is similar to the SDR system. Although only a single R–D link exists in the system, this target relay can be

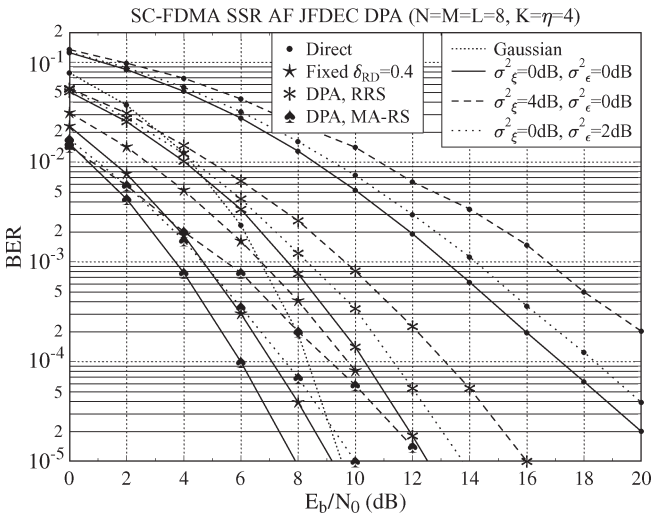

Fig. 8. SSR: BER performance of relay selection schemes that invoke DPA.

selected by considering the position tradeoffs among multiple-source MTs and multiple RCs in an effort to reduce the path loss. Meanwhile, a useful diversity gain is still attainable by relay selection for transmission over Rayleigh fading channels. However, MA-RS considers the single-relay-based support of all K source users, whose signal occupies all the $(K \times N)$ subbands while considering all the $(K \times J)$ possible S–R links. Thus, the selection diversity gain achieved in the presence of deep shadow fading does not improve the link-level reliability quantified in terms of the BER performance. Therefore, the DPA-aided MA-RS allows the system to achieve a BER of 10^{-4} at $E_b/N_0 = 6$ dB when we have $\sigma_\xi^2 = \sigma_\epsilon^2 = 0$ dB. In addition, because the power control determines the transmit power of all source MTs and relays, the corresponding performance differences between $\sigma_\epsilon^2 = 0$ and $\sigma_\epsilon^2 = 2$ are quantified in Figs. 6–8 for the EPA, OPA, and DPA schemes in the presence of both perfect and imperfect power control.

In addition to the aforementioned BER performance analysis, we quantify the sum rate of all user's data transmissions to represent the attainable MU system throughput in terms of the Shannon continuous-input–continuous-output memoryless

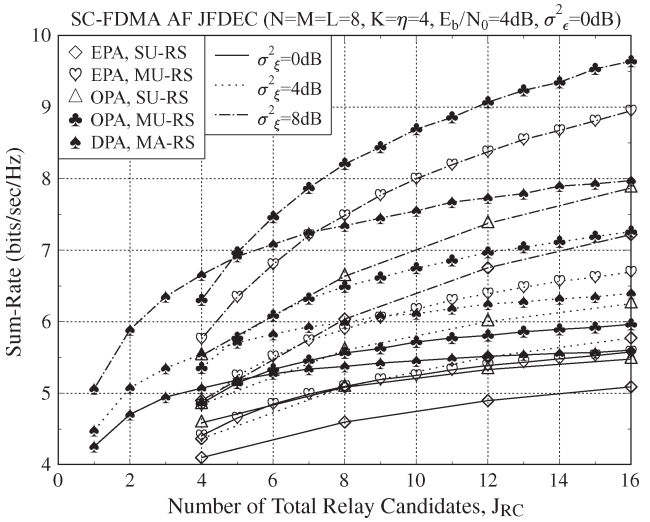

Fig. 9. Effect of varying the number of relay candidates.

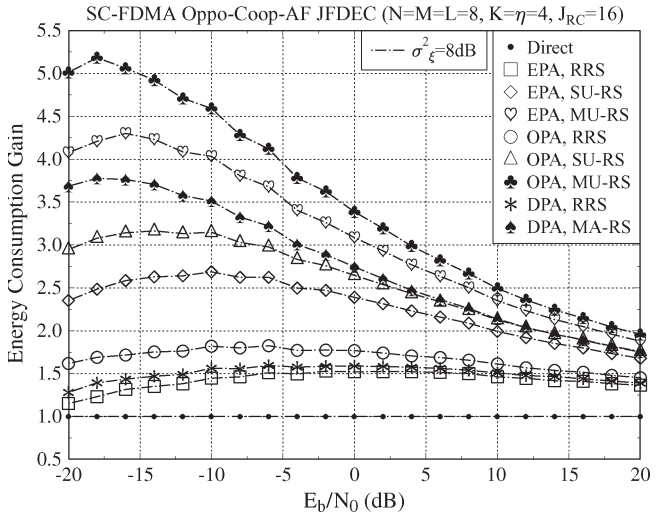

Fig. 10. Energy consumption of the relay selection schemes for 8-dB shadowing variance.

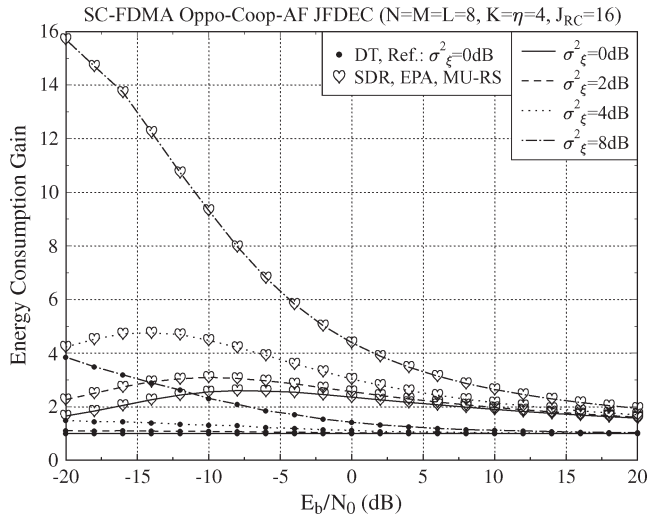

Fig. 11. Shadowing effects on the energy consumption of MU-RS for SDR that invokes EPA.

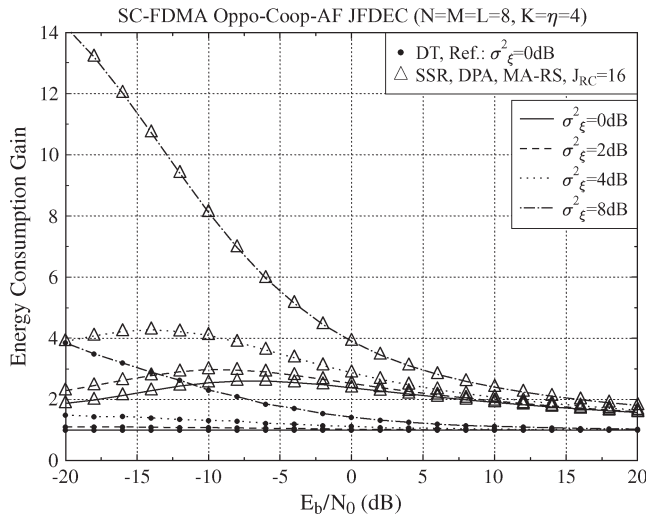

Fig. 12. Shadowing effects on the energy consumption of MA-RS for SSR that invokes DPA.

channel (CCMC) capacity [45]. From a resource management point of view, Fig. 9 depicts the attainable system throughput as a function of the total number of RCs when the number of source MTs was fixed to $K = 4$ and we had $E_b/N_0 = 4$ dB. Observe in Fig. 9 that the sum rate improves upon increasing the number of RCs. In particular, the MU-RS scheme can substantially improve the throughput compared to the SU-RS approach, particularly when communicating over channels subject to shadow fading. Moreover, the sum rate of MA-RS is not unduly affected by varying the number of RCs compared with both the SU-RS and MU-RS schemes. In addition, we note that MA-RS can support OR, even when the number of RCs is $J < K$.

To quantify the attainable energy efficiency when invoking different power sharing and relay selection schemes, Fig. 10 illustrates ECG versus the E_b/N_0 performance of both the SDR and SSR systems for a shadowing variance of 8 dB under perfect power control for SU-RS in conjunction with $J = 4$ and for MU-RS using $J = 16$. Clearly, when aiming for a fixed target E_b/N_0 of, e.g., -10 dB in the presence of shadowing compared with a noncooperative direct transmission scenario, the MU diversity gain accrued from avoiding small-scale fading allows the MU-RS scheme to achieve a significant ECG of 4 for EPA and 4.5 for OPA, whereas SU-RS attains gains of 2.6 and 3.1 for EPA and OPA, respectively. MA-RS obtains a similar ECG as the OPA-aided SU-RS but imposes significantly lower complexity. Finally, RRS has the lowest gain of about 1.5, regardless of the specific power allocation employed.

Furthermore, because we adopt the direct transmission regime in the absence of shadowing as a reference, the shadowing effects imposed on ECG are illustrated in Fig. 11 for MU-RS that invokes EPA and in Fig. 12 for the DPA-aided MA-RS associated with $J = 16$ under perfect power control. The ECG difference between the scenarios associated with different shadowing variances implies that opportunistic scheduling constitutes a power-efficient design when communicating over realistic shadow-fading channels associated with $\sigma_\xi^2 = 0, 2, 4, 8$ dB compared with the noncooperative benchmarkers. In particular, when reducing the transmit power and,

hence, E_b/N_0, the ECGs of both MU-RS and MA-RS are more substantially increased for $\sigma_\xi^2 = 8$ dB compared with the lower fading variances considered. For instance, MU-RS and MA-RS may achieve an ECG of 9 and 8 at $E_b/N_0 = -10$ dB, respectively.

VI. Conclusion

In this paper, we have evaluated the performance benefits of the energy-efficient opportunistic AF cooperation-aided MU SC-FDMA uplink, which was designed to be free from any MUI at the relays when communicating over frequency-selective fading channels in shadow-fading scenarios. The CD-RS schemes were investigated, considering source/relay power sharing based on the proposed JFDEC-MMSE solution, to exploit the MU selective diversity combined with cooperative diversity in the presence of both pass loss and shadowing while subjected to imperfect power control. Our results demonstrate that, at a BER of 10^{-4}, the proposed receiver can save 2-dB power by achieving a higher cooperative diversity gain than the conventional receiver. For instance, when the channel exhibits a shadowing variance of 8 dB at $E_b/N_0 = -10$ dB, an ECG of $2.5 \sim 4.5$ is attainable by invoking the proposed SU-RS, MU-RS, and MA-RS schemes compared with the noncooperative scenario. Most importantly, the ECG gleaned from our MU-RS and MA-RS schemes may increase to $4 \sim 8$ when the shadowing variance is increased from 4 dB to 8 dB, compared with the direct transmission in the absence of shadowing at $E_b/N_0 = -10$ dB.

Appendix

Because we have (22) in Section III-B, all the diagonal elements of $\boldsymbol{A}_{k'}^{\mathrm{t}}$ are equal, which are given by

$$\begin{aligned} a_{k'nn}^{\mathrm{t}} &= \frac{1}{N}\mathrm{Tr}\left[\boldsymbol{A}_{k'}^{\mathrm{t}}\right] \\ &= \frac{1}{N}\sum_{n=0}^{N-1}\left(\left(w_{k',n}^{\mathrm{D}}\right)^{*} h_{0,k',n}^{\mathrm{D,f}} + \left(w_{k',(n+N)}^{\mathrm{D}}\right)^{*} h_{1,k',n}^{\mathrm{D,f}}\right). \end{aligned} \tag{41}$$

The power of the desired signal at any instant is expressed by

$$\begin{aligned} P_{des} &= P_k^{\mathrm{S}}\left(a_{k'nn}^{\mathrm{t}}\right)^2 \\ &= P_k^{\mathrm{S}}\left[\frac{1}{N}\sum_{n=0}^{N-1}\left(\frac{\left|h_{0,k',n}^{\mathrm{D,f}}\right|^2}{\sigma_N^2} + \frac{\left|h_{1,k',n}^{\mathrm{D,f}}\right|^2}{\mathcal{N}_{1,n}^{\mathrm{D}}}\right) e_{k'n}\right]^2. \end{aligned} \tag{42}$$

In parallel, the power of the estimated signal, which is defined as the power of the desired signal plus the power of the ISI, is given by the circulant covariance matrix of the estimated signal $\hat{\boldsymbol{y}}_{k'}^{\mathrm{D,t}}$ as follows:

$$\begin{aligned} P_{est} &= P_{des} + P_{ISI} = \frac{1}{N}\mathrm{Tr}\left\{\mathrm{E}\left[\boldsymbol{A}_{k'}^{\mathrm{t}}\boldsymbol{x}_{k'}^{\mathrm{t}}\left(\boldsymbol{x}_{k'}^{\mathrm{t}}\right)^H\left(\boldsymbol{A}_{k'}^{\mathrm{t}}\right)^H\right]\right\} \\ &= \frac{P_k^{\mathrm{S}}}{N}\sum_{n=0}^{N-1}\left[\left(\frac{\left|h_{0,k',n}^{\mathrm{D,f}}\right|^2}{\sigma_N^2} + \frac{\left|h_{1,k',n}^{\mathrm{D,f}}\right|^2}{\mathcal{N}_{1,n}^{\mathrm{D}}}\right) e_{k'n}\right]^2. \end{aligned} \tag{43}$$

In addition, the desired signal is corrupted by the noise, whose power is given by the diagonal elements of covariance matrix of the equivalent noise at the receiver, yielding

$$\begin{aligned} \hat{\mathcal{N}} &= \frac{1}{N}\mathrm{Tr}\left\{\mathrm{E}\left[\hat{\boldsymbol{n}}_D^{\mathrm{t}}\left(\hat{\boldsymbol{n}}_D^{\mathrm{t}}\right)^H\right]\right\} \\ &= \frac{1}{N}\sum_{n=0}^{N-1}\left(\frac{\left|h_{0,k',n}^{\mathrm{D,f}}\right|^2}{\sigma_N^2} + \frac{\left|h_{1,k',n}^{\mathrm{D,f}}\right|^2}{\mathcal{N}_{1,n}^{\mathrm{D}}}\right) e_{k'n}^2. \end{aligned} \tag{44}$$

Hence, we obtain the overall SINR $\gamma_{k'}$ per bit simplified as follows:

$$\begin{aligned} \gamma_{k'} &= \frac{P_{des}}{P_{ISI} + \hat{\mathcal{N}}} \\ &= \left[\left(\frac{1}{N}\sum_{n=0}^{N-1}\frac{\gamma_{k',n}^{\mathrm{D0}} + \gamma_{k',n}^{\mathrm{D1}}}{\gamma_{k',n}^{\mathrm{D0}} + \gamma_{k',n}^{\mathrm{D1}} + 1}\right)^{-1} - 1\right]^{-1} \\ &= \left(\frac{1}{N}\sum_{n=0}^{N-1}\frac{1}{\gamma_{k',n}^{\mathrm{D0}} + \gamma_{k',n}^{\mathrm{D1}} + 1}\right)^{-1} - 1 \\ &= P_{k'}^{\mathrm{S}} e_{k'}^{-1} - 1. \end{aligned} \tag{45}$$

References

[1] L. Hanzo, O. Alamri, M. El-Hajjar, and N. Wu, *Near-Capacity Multifunctional MIMO Systems: Sphere-Packing, Iterative Detection and Cooperation*. Hoboken, NJ: Wiley, 2009.

[2] A. Sendonaris, E. Erkip, and B. Aazhang, "User cooperation diversity—Parts I and II," *IEEE Trans. Commun.*, vol. 51, no. 11, pp. 1927–1948, Nov. 2003.

[3] R. U. Nabar, H. Bölcskei, and F. W. Kneubühler, "Fading relay channels: Performance limits and space-time signal design," *IEEE J. Sel. Areas Commun.*, vol. 22, no. 6, pp. 1099–1109, Aug. 2004.

[4] P. Anghel and M. Kaveh, "Exact symbol error probability of a cooperative network in a Rayleigh fading environment," *IEEE Trans. Wireless Commun.*, vol. 3, no. 5, pp. 1416–1421, Sep. 2004.

[5] J. N. Laneman, D. N. C. Tse, and G. W. Wornell, "Cooperative diversity in wireless networks: Efficient protocols and outage behavior," *IEEE Trans. Inf. Theory*, vol. 50, no. 12, pp. 3062–3080, Dec. 2004.

[6] W. Fang, L.-L. Yang, and L. Hanzo, "Single-user performance of direct-sequence code-division multiple access using relay diversity and power allocation," *IET Commun.*, vol. 2, no. 3, pp. 462–472, Mar. 2008.

[7] R. Zhang and L. Hanzo, "Coding schemes for energy-efficient multisource-cooperation-aided uplink transmission," *IEEE Signal Process. Lett.*, vol. 16, no. 5, pp. 438–441, May 2009.

[8] L. Wang and L. Hanzo, "The resource-optimized differentially modulated hybrid AF/DF cooperative cellular uplink using multiple-symbol differential sphere detection," *IEEE Signal Process. Lett.*, vol. 16, no. 11, pp. 965–968, Nov. 2009.

[9] Y. Li, B. Vucetic, Z. Zhou, and M. Dohler, "Distributed adaptive power allocation for wireless relay networks," *IEEE Trans. Wireless Commun.*, vol. 6, no. 3, pp. 948–958, Mar. 2007.

[10] M. Kaneko, K. Hayashi, P. Popovski, K. Ikeda, H. Sakai, and R. Prasad, "Amplify-and-forward cooperative diversity schemes for multicarrier systems," *IEEE Trans. Wireless Commun.*, vol. 7, no. 5, pp. 1845–1850, May 2008.

[11] E. C. van der Meulen, "Three-terminal communication channels," *Adv. Appl. Probab.*, vol. 3, no. 1, pp. 120–154, 1971.

[12] A. Bletsas, A. Khisti, D. Reed, and A. Lippman, "A simple cooperative diversity method based on network path selection," *IEEE J. Sel. Areas Commun.*, vol. 24, no. 3, pp. 659–672, Mar. 2006.

[13] Y. Zhao, R. Adve, and T. J. Lim, "Improving amplify-and-forward relay networks: Optimal power allocation versus selection," *IEEE Trans. Wireless Commun.*, vol. 6, no. 8, pp. 3114–3123, Aug. 2007.

[14] A. Bletsas, H. Shin, and M. Z. Win, "Cooperative communications with outage-optimal opportunistic relaying," *IEEE Trans. Wireless Commun.*, vol. 6, no. 9, pp. 3450–3460, Sep. 2007.

[15] R. Madan, N. Mehta, A. Molisch, and J. Zhang, "Energy-efficient cooperative relaying over fading channels with simple relay selection," *IEEE Trans. Wireless Commun.*, vol. 7, no. 8, pp. 3013–3025, Aug. 2008.
[16] Y. Jing and H. Jafarkhani, "Single- and multiple-relay selection schemes and their achievable diversity orders," *IEEE Trans. Wireless Commun.*, vol. 8, no. 3, pp. 1414–1423, Mar. 2009.
[17] H. G. Myung, J. Lim, and D. J. Goodman, "Single-carrier FDMA for uplink wireless transmission," *IEEE Veh. Technol. Mag.*, vol. 1, no. 3, pp. 30–38, Sep. 2006.
[18] *E-UTRA LTE Physical Layer—General Description*, 3GPP Std. TS 35.201 (V8.3.0), 2009.
[19] D. Falconer, S. L. Ariyavisitakul, A. Benyamin-Seeyar, and B. Eidson, "Frequency-domain equalization for single-carrier broadband wireless systems," *IEEE Commun. Mag.*, vol. 40, no. 4, pp. 58–66, Apr. 2002.
[20] N. Benvenuto, R. Dinis, D. Falconer, and S. Tomasin, "Single-carrier modulation with nonlinear frequency domain equalization: An idea whose time has come—Again," *Proc. IEEE*, vol. 98, no. 1, pp. 69–96, Jan. 2010.
[21] F. Pancaldi, G. M. Vitetta, R. Kalbasi, N. Al-Dhahir, M. Uysal, and H. Mheidat, "Single-carrier frequency-domain equalization," *IEEE Signal Process. Mag.*, vol. 25, no. 5, pp. 37–56, Sep. 2008.
[22] L. Hanzo, M. Münster, B.-J. Choi, and T. Keller, *OFDM and MC-CDMA for Broadband Multiuser Communications, WLANs and Broadcasting*. Hoboken, NJ: Wiley, 2003.
[23] H. G. Myung and D. J. Goodman, *Single Carrier FDMA: A New Air Interface for Long Term Evolution*. Hoboken, NJ: Wiley, 2008.
[24] L.-L. Yang, *Multicarrier Communications*. Hoboken, NJ: Wiley, 2009.
[25] J. Zhang, L.-L. Yang, and L. Hanzo, "Multiuser performance of the amplify-and-forward single-relay-assisted SC-FDMA uplink," in *Proc. IEEE 70th VTC—Fall*, Sep. 2009, pp. 1–5.
[26] H. Gacanin and F. Adachi, "A performance of cooperative relay network based on OFDM/TDM using MMSE-FDE in a wireless channel," in *Proc. IEEE 70th VTC—Fall*, Sep. 2009, pp. 1–5.
[27] A. Goldsmith, *Wireless Communications*. Cambridge, U.K.: Cambridge Univ. Press, 2005.
[28] G. Kadel, "Diversity and equalization in frequency domain a robust and flexible receiver technology for broadband mobile communication systems," in *Proc. IEEE Veh. Technol. Conf.*, May 1997, vol. 2, pp. 894–898.
[29] M. V. Clark, "Adaptive frequency-domain equalization and diversity combining for broadband wireless communications," *IEEE J. Sel. Areas Commun.*, vol. 16, no. 8, pp. 1385–1395, Oct. 1998.
[30] A. Gusmao, R. Dinis, and N. Esteves, "On frequency-domain equalization and diversity combining for broadband wireless communications," *IEEE Trans. Commun.*, vol. 51, no. 7, pp. 1029–1033, Jul. 2003.
[31] J. Coon, S. Armour, M. Beach, and J. McGeehan, "Adaptive frequency-domain equalization for single-carrier multiple-input–multiple-output wireless transmissions," *IEEE Trans. Signal Process.*, vol. 53, no. 8, pp. 3247–3256, Aug. 2005.
[32] J.-S. Baek and J.-S. Seo, "Efficient design of block-adaptive equalization and diversity combining for space-time block-coded single-carrier systems," *IEEE Trans. Wireless Commun.*, vol. 7, no. 7, pp. 2608–2611, Jul. 2008.
[33] H. Xiong, J. Xu, and P. Wang, "Frequency-domain equalization and diversity combining for demodulate-and-forward cooperative systems," in *Proc. IEEE ICASSP*, Mar. 2008, pp. 3245–3248.
[34] K. S. Woo, Y. J. Kim, H. I. Yoo, J. Kim, S. Yun, and Y. S. Cho, "An improved receive diversity combining technique for SC-FDMA-based cooperative relays," in *Proc. IEEE 70th VTC—Fall*, Sep. 2009, pp. 1–5.
[35] K. S. Woo, H. Yim, Y. J. Kim, H. I. Yoo, and Y. S. Cho, "An efficient receive-diversity-combining technique for SC-FDMA-based cooperative relays," *IEEE Trans. Veh. Technol.*, vol. 59, no. 8, pp. 4187–4191, Oct. 2010.
[36] N. Kong and L. Milstein, "Error probability of multicell CDMA over frequency-selective fading channels with power control error," *IEEE Trans. Commun.*, vol. 47, no. 4, pp. 608–617, Apr. 1999.
[37] Z. Han, T. Himsoon, W. Siriwongpairat, and K. Liu, "Resource allocation for multiuser cooperative OFDM networks: Who helps whom and how to cooperate," *IEEE Trans. Veh. Technol.*, vol. 58, no. 5, pp. 2378–2391, Jun. 2009.
[38] Y. Ding and M. Uysal, "Amplify-and-forward cooperative OFDM with multiple-relays: Performance analysis and relay selection methods," *IEEE Trans. Wireless Commun.*, vol. 8, no. 10, pp. 4963–4968, Oct. 2009.
[39] K. Vardhe, D. Reynolds, and B. Woerner, "Joint power allocation and relay selection for multiuser cooperative communication," *IEEE Trans. Wireless Commun.*, vol. 9, no. 4, pp. 1255–1260, Apr. 2010.
[40] J. Zhang, L.-L. Yang, and L. Hanzo, "Power-efficient opportunistic amplify-and-forward single-relay-aided multiuser SC-FDMA uplink," in *Proc. IEEE Veh. Technol. Conf.—Spring*, May 2010, pp. 1–5.
[41] C. Han, T. Harrold, I. Krikidis, I. Ku, T. Le, S. Videv, J. Zhang, S. Armour, P. Grant, H. Haas, L. Hanzo, M. R. Nakhai, J. Thompson, and C. Wang, "Green radio: Radio techniques to enable energy-efficient wireless networks," *IEEE Commun. Mag.—Special Issue on Green Communications*, 2011, to be published.
[42] T. S. Rappaport, *Wireless Communications*, 2nd ed. Englewood Cliffs, NJ: Prentice-Hall, 2002.
[43] D. Z. Filho, L. Féty, and M. Terré, "A hybrid single-carrier/multicarrier transmission scheme with power allocation," *EURASIP J. Wireless Commun. Netw.*, vol. 2008, pp. 1–11, 2008.
[44] U. Madhow and M. L. Honig, "MMSE interference suppression for direct-sequence spread-spectrum CDMA," *IEEE Trans. Commun.*, vol. 42, no. 12, pp. 3178–3188, Dec. 1994.
[45] J. G. Proakis, *Digital Communications*, 4th ed. New York: McGraw-Hill, 2000.

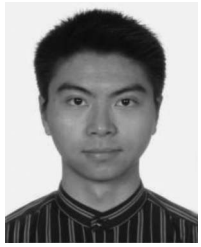

Jiayi Zhang (S'07) received the B.Eng. degree in 2006 from Nanjing University of Aeronautics and Astronautics, Nanjing, China, and the M.Sc. (with distinction) degree in 2007 from the University of Southampton, Southampton, U.K., where he is currently working toward the Ph.D. degree within the Communications Research Group, School of Electronics and Computer Science, and is also involved in the Mobile Virtual Centre of Excellence Core 4 Delivery Efficiency and Core 5 Green Radio projects.

His research interests in wireless communications include energy-efficient cooperative relaying, multicell cooperation, and resource allocation.

Lie-Liang Yang (M'98–SM'02) received the B.Eng. degree in communications engineering from Shanghai TieDao University, Shanghai, China, in 1988 and the M.Eng. and Ph.D. degrees in communications and electronics from the Northern (Beijing) Jiaotong University, Beijing, China, in 1991 and 1997, respectively.

From June 1997 to December 1997, he was a Visiting Scientist with the Institute of Radio Engineering and Electronics, Academy of Sciences of the Czech Republic, Prague, Czech Republic. Since December 1997, he has been with the University of Southampton, Southampton, U.K., where he is a Professor with the School of Electronics and Computer Science. His research has covered a wide range of topics in wireless communications, networking, and signal processing. He has published more than 240 research papers in journals and conference proceedings, is the author or a coauthor of three books, and has published several book chapters. Details about his publications can be found at http://www-mobile.ecs.soton.ac.uk/lly/. He is currently an Associate Editor for the *Journal of Communications and Networks* and the *Security and Communication Networks Journal*.

Dr. Yang is currently an Associate Editor for the IEEE TRANSACTIONS ON VEHICULAR TECHNOLOGY.

Lajos Hanzo (F'04) received the B.S. degree in electronics in 1976, the D.Sc. degree in 1983, and the honorary doctorate *Doctor Honaris Causa* degree in 2009.

During his 34-year career in telecommunications, he has held various research and academic posts in Hungary, Germany, and the U.K. Since 1986, he has been with the School of Electronics and Computer Science, University of Southampton, Southampton, U.K., where he is the Chair in Telecommunications. He is also a Professorial Chair at Tsinghua University, Beijing, China. He has been a coauthor of 20 John Wiley–IEEE Press books on mobile radio communications, totaling more than 10 000 pages. He currently directs an academic research team, working on a range of research projects in wireless multimedia communications sponsored by industry, the Engineering and Physical Sciences Research Council, U.K., the European IST Program, and the Mobile Virtual Centre of Excellence, U.K. He is an enthusiastic supporter of industrial and academic liaison and offers a range of industrial courses. For further information on his research in progress and associated publications, see http://www-mobile.ecs.soton.ac.uk.

Dr. Hanzo is a Fellow of the Royal Academy of Engineering and the Institution of Engineering and Technology. He is also the Governor of the IEEE Communications Society and the IEEE Vehicular Technology Society. He is the Editor-in-Chief of the IEEE Press, has published about 970 research entries on IEEEXplore, acted as the Technical Program Committee Chair of IEEE conferences, presented keynote lectures, and received a number of distinctions.